Supplementary Material

1) Model I-V_{lg} curves

To approximate SWNT-device conductance G as a function of liquid-gate potential V_{lg} we model the Schottky barrier that forms at the SWNT-metal interface to calculate the electronic transport due to tunneling and thermal activation.

First, we calculate the doping energy in the bulk of the SWNT, E_{bulk} (defined as the energy difference between the Fermi-level and the center of the band gap), as a function of applied V_{lg} as explained previously in manuscript ref [24]. Next, we consider the metal-SWNT contact interface, where we assume that the local band bending is given by the electrostatic potential profile in the electrical double layer. Although more accurate descriptions of the interfacial electrochemical potential profile and the ionic arrangement in the electrical double-layer can be used, we assume for simplicity that the electrochemical potential along the length of the SWNT changes exponentially with distance, where the decay constant is taken as the Debeye screening length in solution, λ_{D}.[1] Given the doping level in the bulk, E_{bulk}, the energy of the band gap E_{gap}, and the (effective) work function difference between metal surface and SWNT, ΔW, the energy of the conduction band edge E_{C} as a function of distance x from the contact is:

$$E_C(x,V_{\mathrm{lg}}) = E_{bulk}(V_{\mathrm{lg}}) + \frac{E_{gap}}{2} - \left(E_{bulk}(V_{\mathrm{lg}}) + \Delta W\right)\exp\left(\frac{-x}{\lambda_D}\right) \qquad (1.1)$$

Similarly we can calculate the energy of the valence band edge E_{V}. To calculate the combined thermally activated and tunneling current, $I(V_{\mathrm{lg}})$, we use the Landauer-Buttiker formalism for a one dimensional channel:[2]

$$I(V_{\mathrm{lg}}) = |t|^2 \frac{2e}{h} \int P_t(E, V_{\mathrm{lg}}) \left(f_R(E) - f_L(E) \right) dE \tag{1.2}$$

Where $|t|^2$ is the transmission probability, P_{t} is the tunneling probability, f_R and f_L are the Fermi-Dirac distribution functions for right-moving and left-moving species respectively. For holes and electrons at energies away from band-gap and Schottky barrier, we set $P_{\mathrm{t}} = 1$. For energies E where charge carriers are required to tunnel through source and drain Schottky barriers in order to contribute to electronic transport, we calculate the tunneling probability in the WKB-approximation:

$$P_t(E, V_{\mathrm{lg}}) = \exp(-2 \frac{2}{h} \int_{x=0}^{x=x_t} \sqrt{2 m_{eff} \left(E_C(V_{\mathrm{lg}}) - E \right) x} dx) \tag{1.3}$$

Where $m_{\mathrm{eff}} = E_{\mathrm{gap}}/2\nu_{\mathrm{F}}^2$, with ν_{F} the Fermi-velocity, and x_{t} the tunneling-distance.

Finally, to take into account diffusive transport along the bulk of the SWNT-channel, we use the Drude-like conductance:

$$G_D(V_{\mathrm{lg}}) = \frac{\mu e N_c(V_{\mathrm{lg}})}{L} \tag{1.4}$$

Here μ is the carrier mobility and L is the SWNT length. We evaluate the number of charge carriers that contribute to conduction, N_{c}, as a function of V_{lg} using the nearest neighbor tight-binding approximation for the SWNT density of states, $\rho(E)$.[3]

$$N_c(V_{\mathrm{lg}}) = \int_{-\infty}^{\infty} \rho\left(E - E_{bulk}(V_{\mathrm{lg}}) \right) \left(f_R(E) - f_L(E) \right) dE \tag{1.5}$$

Following equations (1.1) to (1.5), an I-V_{lg} curve can be fully defined by the following set of parameters: diameter d and length L of the SWNT, λ_{D}, V_{hf}, which is defined as the gate potential at which the Fermi-level resides in the center of the band-gap, $|t|^2$, ΔW and μ.

2) Model mechanisms

In Figure 2a-d of the manuscript, we use the model explained above to illustrate changes in I-V_{lg}-curves according to the four different biosensing mechanisms. The black curves in figure 2a-d are identical and have been calculated using the following set of parameters: $d = 2$ nm, $L = 1$ μm, $\lambda_D = 3$ nm, $V_{hf} = 50$ mV, $|t|^2 = 0.27$, $\Delta W = 30$ meV, $\mu = 80000$ cm^2/Vs. The red curves in Figure 2a-d show the change in I-V_{lg}-curves after altering one of abovementioned parameters according to a specific mechanism of biosensing. The red curve in Figure 2a represents the electrostatic gating mechanism and is calculated using $V_{hf} = 0$ mV. The red curve in Figure 2b represents the Schottky mechanism and is calculated using $\Delta W = 0$ meV. The red curve in Figure 2c represents the capacitance mechanism where the gate coupling is reduced due to a reduction of the electrostatic capacitance. We used a 89% reduced electrostatic capacitance, which roughly corresponds to 90% of the SWNT being covered with proteins with permittivity, $\varepsilon = 10$, and diameter = 6 nm. Finally, the red curve in Figure 2c represents the mobility mechanism and is calculated using $\mu = 1600$ cm^2/Vs.

3) Horse-heart cytochrome-c adsorption on SWNT-device

\

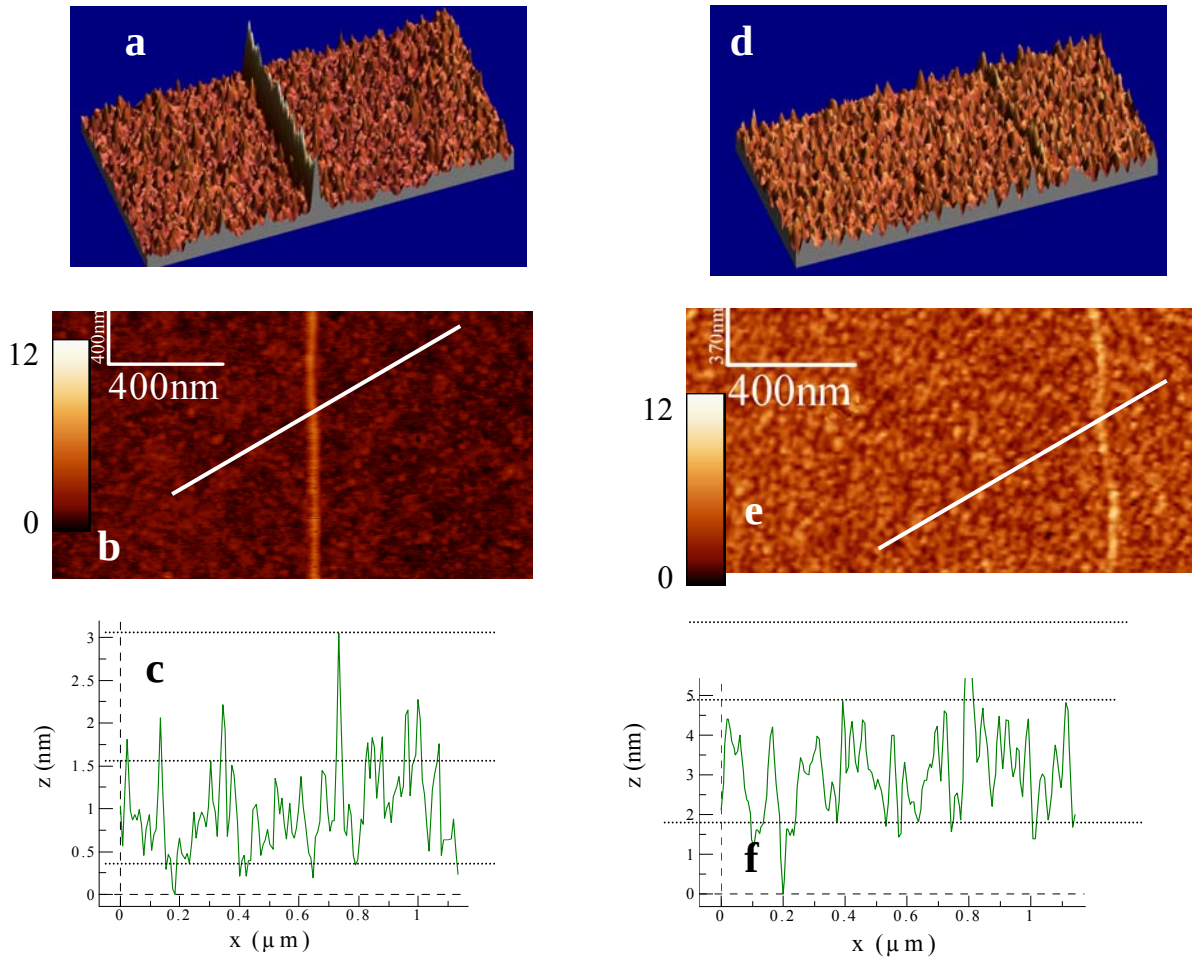

Figure S1. AFM images of cytochrome-c adsorption on a SWNT and SiO_2. (a) and (d) show three-dimensional and (b) and (e) two-dimensional representations of an AFM-topography image of a bare SWNT on a SiO_2 substrate (a and b), and the same SWNT after coating with HHCC (d and e). (c) and (f) show height profiles along the lines as drawn in (b) and (e) respectively.

4) Scatterplot of changes in hole conduction and electron conduction

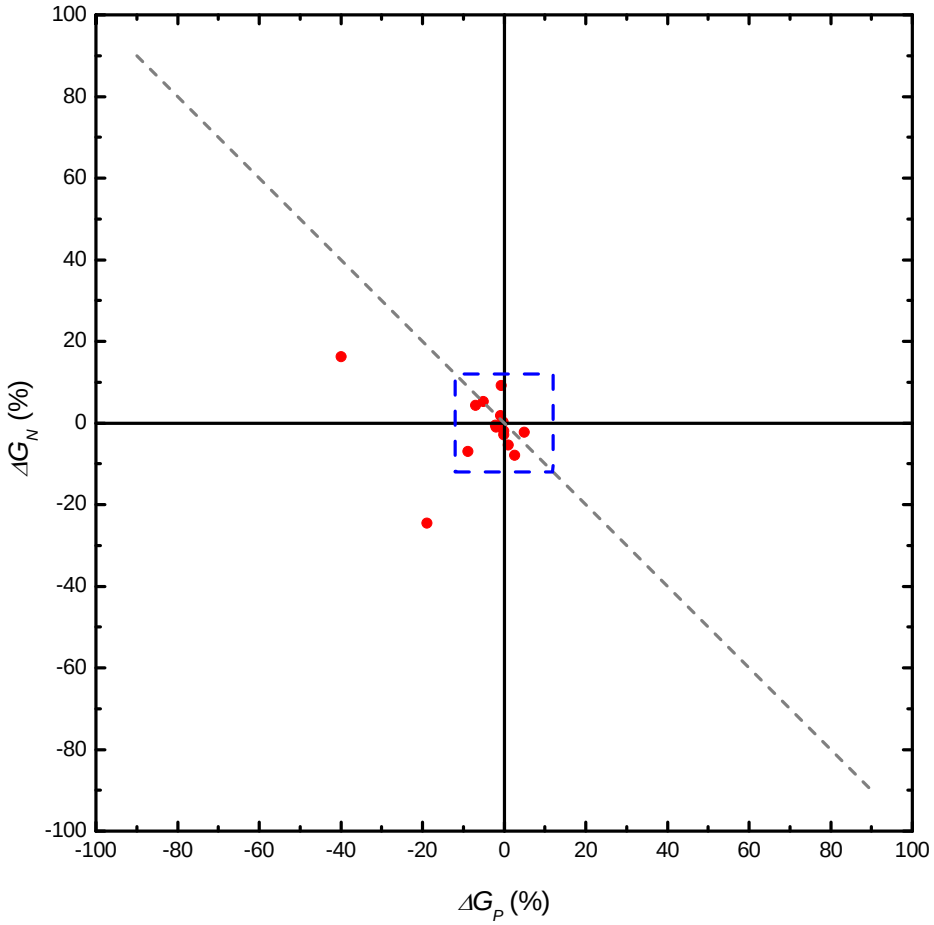

Figure S2. Scatterplot of changes in n-conduction versus changes in p-conduction showing the dataset of manuscript figure 3d on a larger range. The blue rectangle indicates the range as used in the manuscript Figure 3d.

5) Example of Schottky barrier effect after adsorption of antibodies[4]

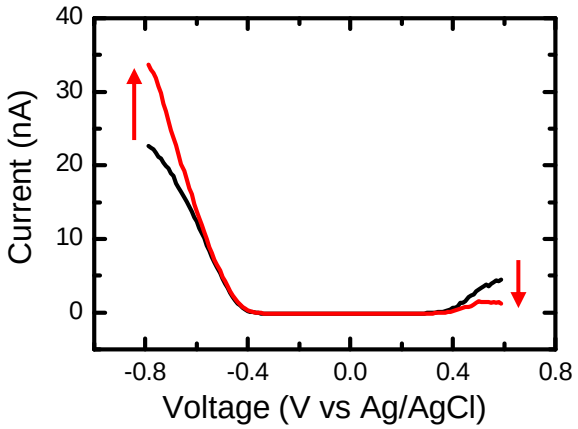

Figure S3. Adsorption of anti-fullerene antibodies on a SWNT-device. The black and red curves show liquid-gate sweeps in PBS and after adsorption of 1.25 µg/ml anti-fullerene antibodies in PBS.[4]

6) Analysis V_{shift}, ΔG_P and ΔG_N for adsorption of HHCC.

To extract V_{shift} from the I-V_{lg} curves before and after adsorption of HHCC, we use a numerical nonlinear least-squares fitting procedure: The sum of squared differences between the $\log[I_{sd}(V_{lg})]$ values as measured before and after HHCC adsorption is minimized with respect to a value V_{shift} by which the two experimental curves are offset with respect to each other along the V_{lg} axis. The use of the logarithm of the I_{sd} values puts equal weight on the current values close to the band gap, such that the impact of small asymmetric conductance changes due to the Schottky barrier mechanism on the resulting value of V_{shift} is small. A histogram of the values obtained for V_{shift} is shown in the manuscript in Figure 3c. After correcting the curves for V_{shift}, we compare the I_{sd} values at the opposite endpoints of the gate-voltage range to calculate ΔG_P and ΔG_N as plotted in manuscript Figure 3d.

In the manuscript we use the method of analysis explained above, only using values for device conductance at the opposite endpoints of the gate-voltage range to calculate ΔG_P

and ΔG_N. We chose not to calculate ΔG_P and ΔG_N based on the entire gate voltage range, for two reasons: First, none of the previously suggested sensing mechanisms predicts that ΔG_P and ΔG_N are independent of gate voltage. Second, for devices that consist of more than one SWNT the shape of the I-V_{lg} curve near the band-gap is a complex function of the properties of the different SWNTs, in which case the most correct way of analyzing ΔG due to Schottky-barrier effects is as far away from the gap as possible. For completeness though, here we do provide a 3-parameter least-squares fit of V_{shift}, ΔG_P and ΔG_N based on the entire gate-voltage range, which qualitatively yields the same results as in Figure 3c and 3d of the manuscript: In this alternative analysis method we multiply all values to the left/right (more negative/positive V_{lg}) of the center of the band gap by $\Delta G_{P/N}$, plus offset the curves by V_{shift} along the V_{lg} axis. Minimizing the sum of squared differences with respect to V_{shift}, ΔG_P and ΔG_N now yields a best fit. The errors in the fit parameters are obtained from the covariance matrix at the best fit solution. Figure S4 shows the results of this alternative fitting method.

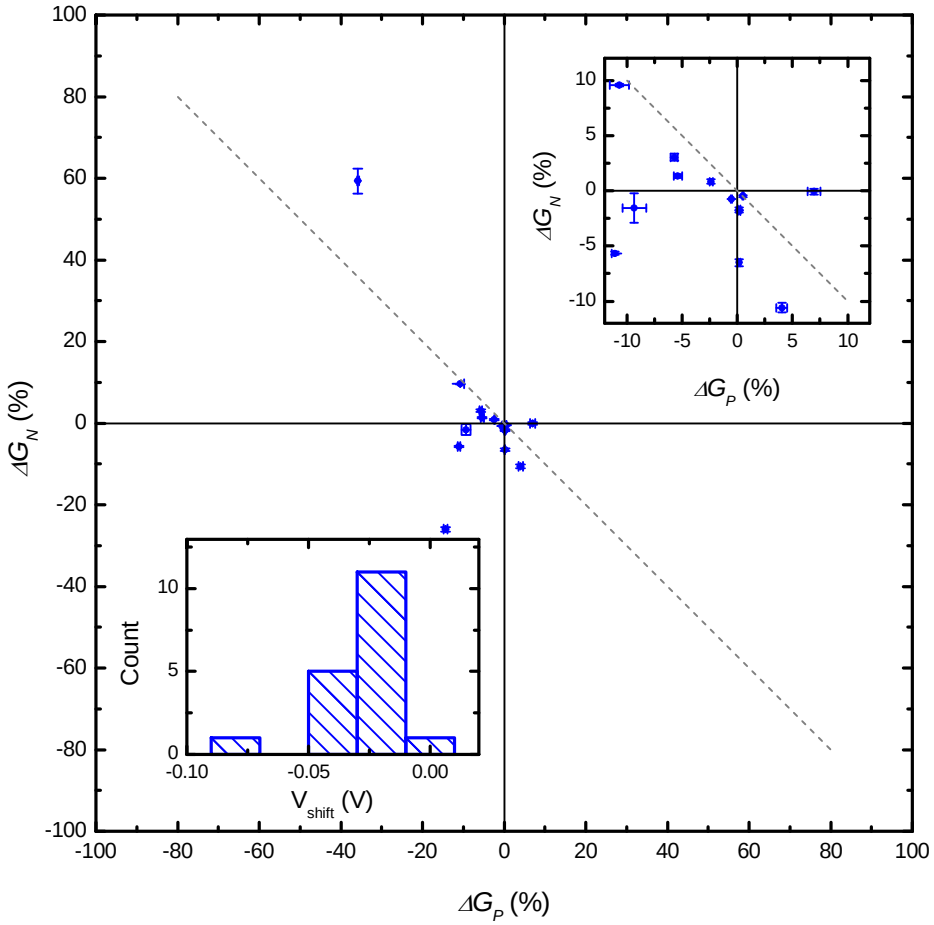

Figure S4. Scatterplot of changes in n-conduction (ΔG_N) versus changes in p-conduction (ΔG_P) as obtained from the 3-parameter least-squares fit of V_{shift}, ΔG_P and ΔG_N as explained in the text. The upper right inset shows the same dataset on a smaller ΔG_P and ΔG_N range. The lower left inset shows a histogram of the obtained values for V_{shift}. The results are essentially the same as for the 1-parameter fit discussed in the main text.

7) Modeling I-V_{lg} curves of HHCC adsorption data

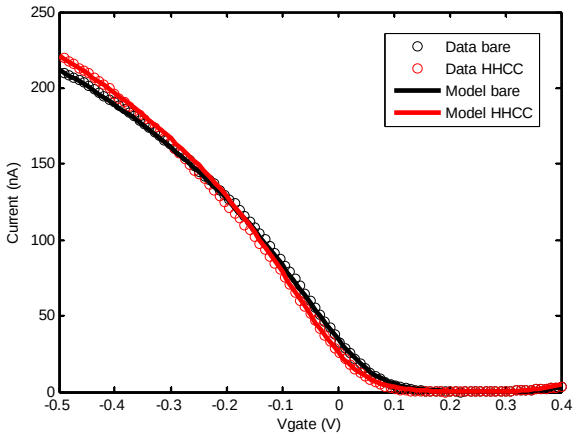

Figure S5. Modeling the adsorption of HHCC on a SWNT-device. The red and black circles correspond to the experimental I-V_{lg}-curves before and after HHCC adsorption as presented in figure 1c of the manuscript. The solid red and black lines are calculated using the model presented previously in this supplementary material. The parameters used to calculate the black curve are d = 1.8 nm, L = 1 µm, λ_D = 3 nm, V_{hf} = 250 mV, $|t|^2$ = 0.27, ΔW = 22 meV, μ = 80000 cm^2/Vs. The red line can be obtained from the same parameters used for the black curve by changing V_{hf} by -33 mV and ΔW by 16 meV (i.e. V_{hf} = 217 mV, ΔW = 38 meV).

References

1. Bard, A. J. & Faulkner, L. R. *Electrochemical Methods: Fundamentals and Applications.* (John Wiley & Sons, New York, 2001).

2. E. D. Minot, *Tuning the Band Structure of Carbon Nanotubes. PhD thesis*, (Cornell University, Ithaca, 2004).

3. Mintmire, J. W. & White, C. T. Univeral density of states for carbon nanotubes. *Phys. Rev Lett.* **81**, 2506-2509 (1998).

4. Erlanger, B. F., Chen, B. X., Zhu, M. & Brus, L. Binding of an anti-fullerene IgG monoclonal antibody to single wall carbon nanotubes. *Nano Lett.* **1,** 465-467 (2001).